RESEARCH ARTICLE

ADVANCED
NANOBIOMED
RESEARCH
Open Access

www.advnanobiomedres.com

In-Gel Generated Palladium Nanostructures as Bioorthogonal Uncaging Reactors

Aisling McGuigan, Víctor Sebastián,* Asier Unciti-Broceta, Jesús Santamaría, and Ferry Melchels*

In the quest to alleviate the severe side effects of chemotherapy, a promising approach is through prodrugs, an inactivate form of the drug that is administered systemically but activated locally. Bioorthogonal chemistry has the potential to generate high doses of drug at the tumor site with minimal off-target exposure. To harness the potential of bioorthogonal prodrugs, implantable heterogenous catalysts consisting of biocompatible polymers with immobilized metal nanoparticles are required. Polymers based on poly(2-hydroxyethyl methacrylate) with different levels of hydrophilicity are functionalized with either palladium nanocubes ($\approx$10 nm) or palladium nanosheets (<200 nm). Using a palladium-sensitive fluorogenic model compound, propargylated resorufin, the nanosheets show higher catalytic activity than the nanocubes, as well as better metal retainment within the hydrogels. The more hydrophilic polymers show improved diffusion, conversion, and release and better recyclability. Converted product is sequestered by the polymer and released with delay, establishing a potential route to sustained release. These heterogenous catalysts can facilitate the clinical translation of bioorthogonal prodrugs.

1. Introduction

Bioorthogonal reactions are those which take place in a biological environment, without interacting or interfering with any biological processes.[1] They facilitate the study of biological processes in living systems, but they also hold promise for targeted drug delivery. Bioorthogonal prodrugs are molecules with little or no pharmacological activity, which are converted into the active parent drug locally upon interacting with an abiotic catalyst such as transition metal, (i.e., palladium (Pd), gold (Au), platinum (Pt), and their alloys, including PdPt, AuPd, and AuPt).[2] The use of bioorthogonal prodrugs combined with a catalytic implant could allow high doses of active drug to be generated locally. This aims to reduce off-target effects associated with gold standard small molecule-based chemotherapy, while still bearing the advantages of small molecules over more complex macromolecules, nanoparticles, and biologics, such as cost, reproducibility, storage stability, and delivery.

A range of bioorthogonal prodrugs have been developed based on common chemotherapeutics such as 5-fluorouracil,[3,4] gemcitabine,[5] irinotecan,[6] floxuridine,[7] doxorubicin,[8] or β-lapachone.[9] These have been demonstrably reverted to the active drug, using a Pd-catalyzed reaction, in vitro and in vivo.

These developments would be of no benefit without concurrent developments in the delivery of the Pd-trigger to the location

A. McGuigan, F. Melchels
Institute of Biological Chemistry
Biophysics and Bioengineering
School of Engineering and Physical Sciences
Heriot-Watt University
Edinburgh EH14 4AS, UK
E-mail: ferry.melchels@unisa.edu.au

V. Sebastián, J. Santamaría
Instituto de Nanociencia y Materiales de Aragon (INMA)
CSIC-Universidad de Zaragoza
Campus Rio Ebro, Edificio I+D, C/ Poeta Mariano Esquillor, s/n, Zaragoza
50018, Spain
E-mail: victorse@unizar.es

The ORCID identification number(s) for the author(s) of this article can be found under https://doi.org/10.1002/anbr.202500118.

V. Sebastián, J. Santamaría
Department of Chemical and Environmental Engineering
University of Zaragoza
Campus Rio Ebro, C/María de Luna, 3, Zaragoza 50018, Spain

V. Sebastián, J. Santamaría
Networking Research Center in Biomaterials
Bioengineering and Nanomedicine (CIBER-BBN)
Instituto de Salud Carlos III
Madrid 28029, Spain

A. Unciti-Broceta
Edinburgh Cancer Research
Cancer Research UK Scotland Centre
Institute of Genetics and Cancer
University of Edinburgh
Edinburgh EH4 2XR, UK

F. Melchels
Future Industries Institute
University of South Australia
Mawson Lakes SA 5095, Australia

**ADVANCED
SCIENCE NEWS**

www.advancedsciencenews.com

**ADVANCED
NANOBIOMED
RESEARCH**
Open Access

www.advnanobiomedres.com

where it is needed. Biocompatible catalytic Pd nanomaterials have been engineered in or on various organic, inorganic, or bio-derived materials. Nano-, micro-, or macroscale Pd devices have been reported enabling control over whether the prodrug is activated intracellularly[10–12] or extracellularly.[13] Supported heterogeneous catalytic systems offer attractive advantages in terms of a balance between reactivity, biocompatibility, and spatiotemporal control. To date, the polymer bases for the Pd-functionalized implants have mostly been nano- or micro-sized polystyrene or polystyrene-poly(ethylene glycol) beads.[10,13,14] Although these sizes are useful for studies in small zebrafish embryos,[5,13] and for direct injection into mouse tumor xenografts,[4,8] control over their dosage, location, and mobility once injected remains a challenge.

To this end, the use of bulk hydrogels for the immobilization of the relevant Pd catalysts and application to prodrug activation has been reported, using biodegradable alginate and agarose hydrogels.[15] While the combined biocompatibility of hydrogels and catalytic functionality of Pd nanoparticles facilitate localized prodrug activation,[4,16] the biodegradability of these hydrogel materials raises concerns about the fate of the entrapped Pd upon material degradation. Therefore, the development of nondegradable hydrogel-based heterogeneous catalysts would bear advantages including ease of handling and delivery in the form of an implant, alongside enhanced stability, reusability, and traceability.

Besides the selection of an appropriate hydrogel, the enhancement of catalytic activity by control of the nanoparticle shape provides an attractive option to use in catalytic implant design. Different shapes have different active surface areas and display facets that often present different catalytic behavior and/or sensitivity to deactivation by ambient molecules, something that can be very important in biological environments. It is also clear that enhancing the catalytic activity of the entrapped Pd catalysts would reduce the amount of Pd required in the implant to facilitate efficient and useful prodrug conversions.

Palladium nanocubes (PdNC) have been reported to have enhanced catalytic activity compared with their spherical counterparts.[17] Moreover, they have been previously investigated as anticancer treatments, reportedly inducing apoptosis in HeLa cell culture, although high sensitivity to surface fouling in the presence of biomolecules suggested the requirement of an appropriate delivery system.[18,19] Immobilization of PdNC in hydrogels can aid their protection from potential biofouling.[2] The synthesis of PdNC in solution is well established,[20–23] utilizing the weak reducing agent L-ascorbic acid (L-AA) in the presence of bromide ions as a stabilizer; however, there have been no reports yet of the synthesis of Pd nanocubes in situ in hydrogels. Synthesis of nanoparticles in situ in a preformed hydrogel could improve stability and longevity of the nanoparticle catalytic activity, while simplifying the process of preparing catalytic implants.

Palladium nanosheets (PdNS) form another attractive nanostructure for catalysis. We recently reported a novel method for PdNS inside poly lactic-co-glycolic acid (PLGA) nanoparticles[24] and demonstrated catalytic activity of PdNS immobilized in exosomes[12,25] as well as alginate and agarose hydrogels.[15] This synthetic approach is based on the gas-phase reduction of Pd(II) precursor loaded into the carrier during its synthesis. Carbon monoxide (CO) is used as the gas phase, serving as both a mild reducing agent and a capping agent, promoting the anisotropic growth of these bidimensional metallic nanosheet structures of only 10 atomic layers thick.[26,27] Another advantage of the CO reduction method is the absence of chemical contamination from the reductant; the gas is simply vented at the end of the reaction. The use of CO as a reducing agent not only ensures a contaminant-free synthesis but also facilitates homogeneous in situ PdNS formation within porous hydrogels, as the gas can easily diffuse through the matrix, promoting a homogeneous distribution of PdNs. The high surface area PdNS are capable catalysts for the depropargylation reaction for activation of prodyes and prodrugs under biorelevant conditions.[15]

In this work, we explore the in situ preparation of Pd nanocubes and nanosheets inside hydrogels based on poly(2-hydroxyethyl methacrylate) (pHEMA). HEMA monomer was copolymerized with acrylamide in different ratios to achieve different levels of hydrophilicity. Synthetic methods reported to achieve specific nanostructures were adopted to allow in situ formation inside the hydrogels. Nanoparticle shape, distribution, and loading were confirmed, and the influence of nanoshape and hydrogel hydrophilicity on catalytic activity, release kinetics, recycling, and Pd leaching was assessed.

2. Results

### 2.1. Pd Nanostructures are Formed within Hydrogels

PdNC were first prepared in solution by a previously reported method,[20] using cetyltrimethylammonium bromide (CTAB) as a capping agent to control cube size and shape, and L-ascorbic acid (L-AA) as the reductant. This resulted in solely cube-shaped nanoparticles with an edge length of 11.6 $\pm$ 2.2 nm (**Figure 1**d). This method was then adapted and applied to pHEMA-GG and pHEMA-co-AM. The Pd(II) precursor was first left to diffuse overnight into the hydrogel discs, which turned from white to yellow. The discs were transferred to a solution of CTAB and heated to 95 °C for 1 h, inducing a color change from yellow to a light red/brown. Upon the addition of reductant L-AA, the solution rapidly turned dark brown. The resultant discs were a nonhomogeneous light brown color (Figure 1a). The second approach omitted the CTAB reagent to reduce potential loss of Pd precursor to the CTAB solution, with the hypothesis that a capping agent might not be required within the confined spaces inside the hydrogel. The hydrogel discs were immersed in the Pd precursor solution overnight, then heated to 95 °C within that solution. This method produced discs that were darker brown after heating, indicating higher uptake of the Pd(II) precursor than the first approach. Upon addition of L-AA, the solution containing the discs rapidly turned black; collected discs were homogeneously black and metallic, which was expected for the reduction of Pd(II) to Pd(0). The visual improvement was corroborated by improved catalytic conversion ability of PdNC-laden pHEMA-GG prepared without CTAB (Figure 1c). Similar to the solution method, the adapted method yielded Pd nanocubes with an edge length 10.1 $\pm$ 2.9 nm within the pHEMA-GG hydrogel, with some triangular nanostructure by-products (Figure 1b). The method was repeated for the pHEMA-co-AM copolymer with the same outcome.
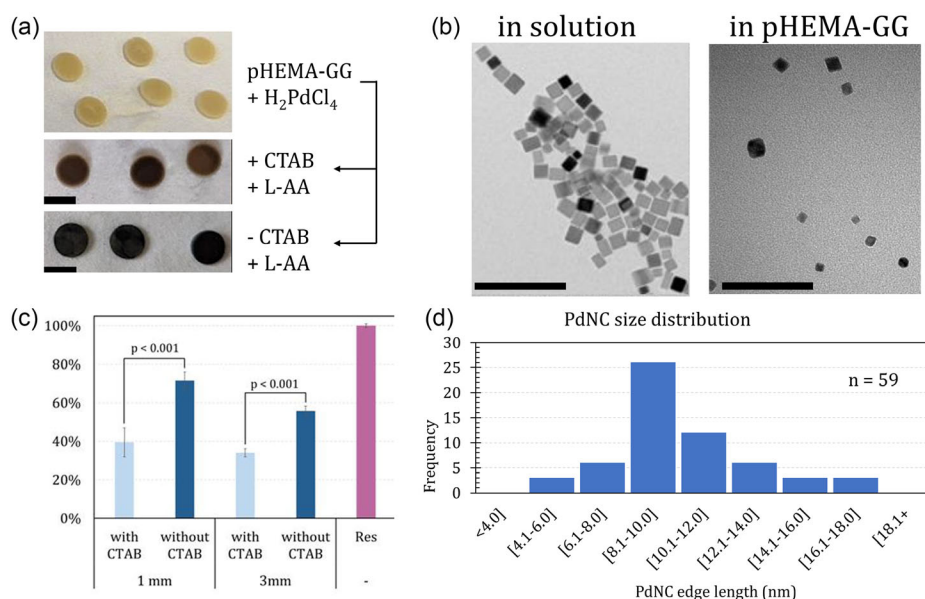
Figure 1. In situ preparation of palladium nanocubes (PdNC) inside pHEMA-GG hydrogels through adaptation of a solution-based protocol. a) Palladium precursor solution diffused into pHEMA-GG hydrogels that turned brown/black upon reduction with L-AA, with or without prior heating in CTAB solution. b) TEM images show similar size and morphology of PdNC inside pHEMA-GG hydrogels compared with PdNC prepared in solution. The pHEMA-GC hydrogel was ultramicrotomed to obtain thin sections suitable for TEM imaging. c) Conversion of proresorufin by pHEMA-GG-PdNC discs prepared by both methods; omission of CTAB improved conversion. d) Particle size (edge length) distribution of PdNC. Scale bars (a) 6 mm and (b) 100 nm.

The protocol for functionalization of exosomes with Pd nanosheets[25] was adapted and applied to functionalize pHEMA-based hydrogel discs. Hydrogel discs were soaked in aqueous Pd(II) precursor, resulting in red-orange hydrogel discs. Upon exposure to CO gas at moderate temperature (60 °C) and 6 bar of pressure, the discs turned black, indicating the reduction of Pd(II) to Pd(0) (**Figure 2**a).

High-angle annular dark-field scanning transmission electron microscopy (HAADF-STEM) was used to observe the Pd nanostructures formed within pHEMA-GG hydrogel discs. The structures visualized in white, indicative of a relatively high atomic mass, were confirmed as Pd using energy-dispersive X-ray spectroscopy (EDX, Figure 2c). The 2D ultrathin nature of the nanostructures observed in earlier studies[25] was reproduced, albeit
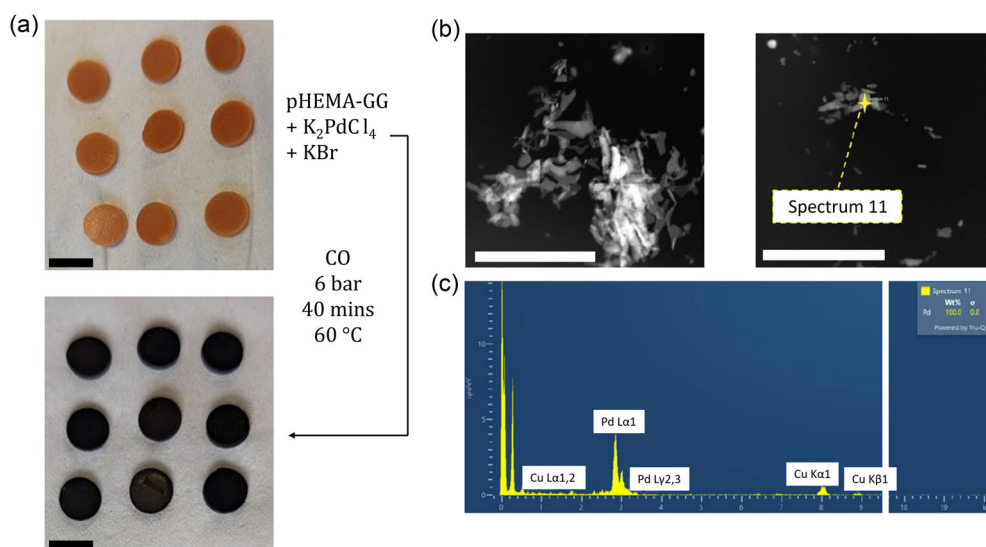
Figure 2. In situ preparation of palladium nanosheets (PdNS) inside pHEMA-GG hydrogels. a) Hydrogels loaded with palladium precursor turn black after reduction of palladium with CO. b) HAADF-STEM images of in situ prepared PdNS in pHEMA-GG. Palladium is visualized in white, showing 2D amorphous sheets of palladium entangled within the pHEMA network. The pHEMA-GC hydrogel was ultramicrotomed to obtain thin sections suitable for TEM imaging. c) EDX spectra confirming the presence of palladium within the structures (spectrum taken at location marked with yellow star in (b)). Scale bars (a) 6 mm and (b,c) 200 nm.

**ADVANCED
SCIENCE NEWS**

www.advancedsciencenews.com

**ADVANCED
NANOBIOMED
RESEARCH**
Open Access

www.advnanobiomedres.com

with highly irregular shapes (Figure 2b). The irregular, flake-like appearance impeded the exact measurement of the dimensions of individual particles; however, their size was within the submicron range and many particles were smaller than 100 nm. Also, it should be noted that the preparation by cryomicrotomy may have influenced the irregular appearance of the Pd nanosheets, as they grow throughout the entire volume of the hydrogel in all directions. This 3D distribution within the hydrogel matrix can lead to variations in the observed cross-sections, giving the impression of irregularity in TEM images.

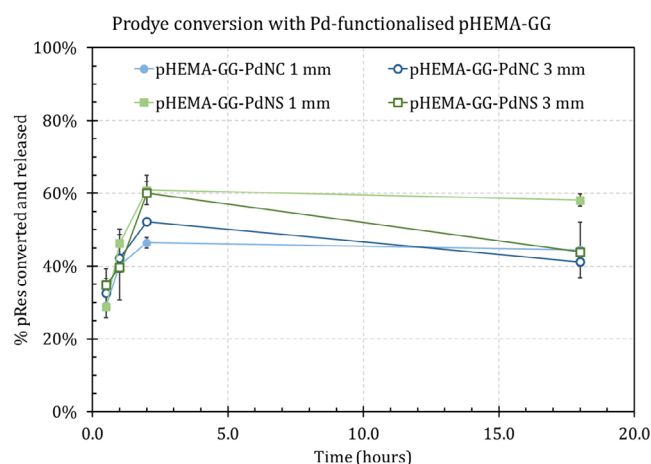## 2.2. Kinetics of Catalytic Conversion and Release from Pd-Laden Hydrogels

The catalytic activity of the Pd-laden hydrogels was assessed using the nonfluorescent prodye proresorufin, where a depropargylation reaction in the presence of Pd converts it to resorufin, a fluorescent pink dye. Resorufin is the same compound detected in the resazurin (alamarBlue) assay for cell metabolic activity. This reaction models the activation of previously developed Pd-labile chemotherapeutic prodrugs. PdNC- and PdNS-laden pHEMA-GG discs both catalyzed the bioorthogonal uncaging reaction, as measured by the concentration of resorufin in the supernatant versus the initial concentration of proresorufin (**Figure 3**).

For all conditions, a maximum was observed at 2 h. This was followed by a decrease in resorufin concentration at the 18 h timepoint, indicative of a reuptake of dye back into the hydrogels. This effect was much more pronounced for the 3 mm thick hydrogel disc than for the 1 mm thick hydrogel discs (Figure 3, open versus closed symbols); the thick discs have threefold greater hydrogel volume to act as a sink for the dye product. Although the 3 mm thick discs also have more Pd available to catalyze the reaction, the small difference in activity

between 1 and 3 mm discs indicates that the extra Pd, which resides deeper into the thicker hydrogel, does not contribute significantly and most of the reaction happens at or near the surface of the disc, that is, the process is diffusion limited. When comparing PdNP shapes, PdNS-laden discs demonstrated higher conversions than PdNC-laden discs at both thicknesses and all time points, inferring a higher activity of these nanoparticles despite the ≈40% lower Pd load (Table 1, Supporting Information). After 2 h, $61 \pm 4\%$ and $60 \pm 3\%$ of proresorufin was converted and released as resorufin by 1 and 3 mm PdNS-laden discs, and for PdNC-laden discs, $46 \pm 1\%$ and $52 \pm 1\%$ was converted and released, respectively.

To assess the influence of hydrophilicity on heterogeneous catalysis, HEMA was copolymerized with acrylamide in two monomer ratios: 1:1.83 and 1:2.75. As expected, acrylamide significantly increased the hydrophilicity as seen from an increase in equilibrium swelling ratio (calculated as the mass ratio in swollen and dried state) from 2.00 ± 0.02 (pHEMA-GG) to 4.16 ± 0.08 (pHEMA-co-AM 1:1.83) and 4.70 ± 0.16- (pHEMA-co-AM 1:2.75). Functionalization with Pd resulted in a small but significant reduction (3%–13%) in swelling rates (Figure 1, Supporting Information).

Copolymers were functionalized with Pd nanostructures using the procedures described above. When used for the catalytic uncaging of proresorufin, the more hydrophilic pHEMA-co-AM gels showed several differences compared with the more hydrophobic pHEMA-GG gels (**Figure 4** versus Figure 3). First, rates of conversion and release were higher for the copolymers, with the differences between PdNS and PdNC being more pronounced up to 2 h. There appeared little difference in proresorufin converting capacity between the two molar ratios of HEMA:AM (1:1.83 and 1:2.75, filled versus open symbols in

Figure 3. Catalytic conversion and release with in-gel generated Pd nanostructures in pHEMA-GG, showing higher catalytic activity for PdNS (green) versus PdNC (blue) and increased re-uptake of dye product with increased hydrogel thickness (light color 1 mm; darker color 3 mm). Catalytic conversion and release expressed as resorufin in the supernatant as a percentage of proresorufin initially offered. $N = 3$ discs $\times$ 3 fluorescence measurements $= 9$ measurements.
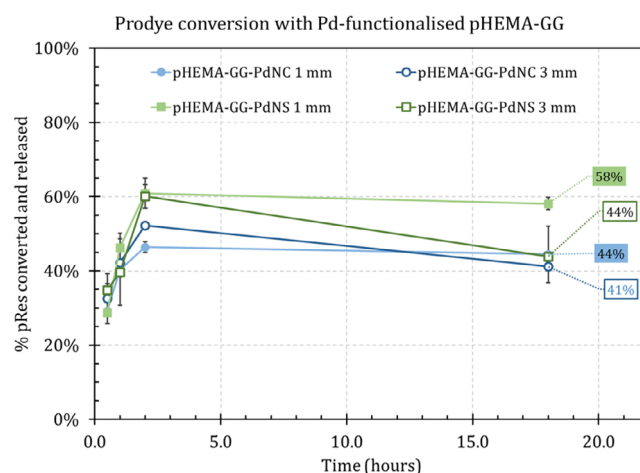
Figure 4. Catalytic conversion and release with in-gel generated palladium nanostructures in pHEMA-co-AM, showing higher catalytic activity for PdNS (green) versus PdNC (blue), and reduced re-uptake of dye product into these hydrophilic hydrogels compared with the more hydrophobic pHEMA-GG (Figure 3). Molar ratios of HEMA:AM of 1:1.83 (open symbols) and 1:2.75 (closed symbols) showed similar profiles. Catalytic conversion and release expressed as resorufin in the supernatant as a percentage of proresorufin initially offered. $N = 2$ discs $\times$ 3 fluorescence measurements $= 6$ measurements.

Figure 4), apart from one timepoint (PdNS at 2 h). Second, the final resorufin concentration after 18 h was much higher for the copolymers than for the pHEMA-GG, with an increase of 22–24% for PdNC and of 14% for PdNS. This could indicate higher catalytic ability for Pd within the copolymer than within pHEMA-GG, though lower reuptake of resorufin is likely the main contributor.

2.3. Release of Sequestered Dye Product from Pd-Laden Hydrogels

To confirm the reuptake of dye into the Pd-laden hydrogels, the discs used for 0.5, 1, and 2 h prodye conversions were left in PBS for 5 days, followed by another 10 days in fresh PBS. This allowed any sequestered dye to be leached out, and not-yet-converted prodye inside the hydrogel to be converted into dye and released. Considerable amounts were leached from the discs; 12–22% of the originally supplied prodye across all conditions (**Figure 5**). This means that the percentages of converted and release prodye presented earlier (Figure 3 and 4) underestimated the efficacy of the catalyst. The actual total amounts of converted dye eventually released after 2 h exposure to proresorufin ranged from $60 \pm 2\%$ for PdNC in pHEMA-co-AM 1:1.83 (increased from $46 \pm 1\%$) to $100 \pm 1\%$ for PdNS in pHEMA-co-AM 1:2.75 (increased from $79 \pm 3\%$).

As could be expected, the amounts of sequestered dye released showed little dependence on Pd nanoshape, but clear differences between the two polymers indicate that this phenomenon is governed by polymer-dependent mass transport, rather than by Pd-dependent catalysis.

The proportion of sequestered dye released from pHEMA-GG discs significantly increased from 12.6 to 21.1% (averaged over both thicknesses and Pd nanoshapes) when exposure time to proresorufin increased from 0.5 to 2 h. In contrast, there was no statistical difference between the proportion of sequestered dye released from pHEMA-co-AM copolymers with increased prodye exposure time (Figure 5). This suggests that the uptake of prodye into the pHEMA-co-AM copolymers is faster than into pHEMA-GG, indicating a positive correlation between diffusion and hydrophilicity.

When comparing the amounts of dye released in the initial 5-day period versus the second 10-day period, pHEMA-GG discs held on to a larger proportion of the sequestered dye than pHEMA-co-AM discs; the proportion of dye released in the second 10-day period averaged 5.5 and 3.0% respectively. This implies that the dye has a higher affinity for pHEMA-GG than for pHEMA-co-AM, as a higher amount of dye stayed behind in the pHEMA-GG discs than in the pHEMA-co-AM discs when equilibrium was reached, or approached, after the initial 5 days of leaching.

No differences were seen between the copolymers with different monomer ratios. The release of dye from copolymers with PdNS was slightly (but significantly) higher than for PdNC-loaded copolymers, which was most likely due to the higher catalytic activity of PdNS leading to a higher amount of dye being stored in the discs when taken out of the prodye solution.

2.4. Amount and Rate of Dye Uptake Depends on Polymer Hydrophilicity

To further untangle the compound effect of catalytic conversion and product reuptake observed in the kinetic experiments, resorufin uptake was assessed separately. Swollen Pd-free hydrogel discs left in a resorufin solution turned pink over time, eventually
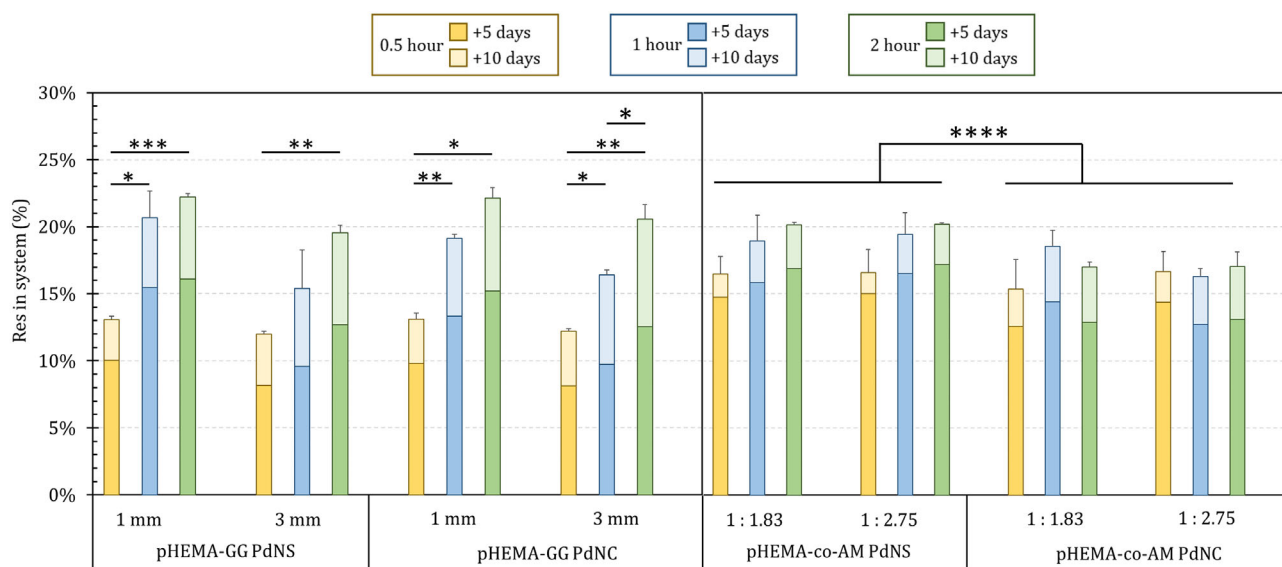
Figure 5. Leaching of sequestered dye showing considerable storage capacity of the dye within the gels. Resorufin released during the 5 + 10 days after prodye conversion experiments showing a higher affinity of the dye for pHEMA-GG than for pHEMA-co-AM hydrogel discs, independent of palladium nanoshape (PdNS versus PdNC). Release of sequestered dye expressed as resorufin in the supernatant as a percentage of proresorufin initially offered. $N = 2$ discs $\times$ 3 fluorescence measurements $= 6$ measurements per timepoint; errors are cumulative across all 12 measurements per stacked column. * $p < 0.05$; ** $p < 0.01$; *** $p < 0.001$; **** $p < 0.0001$.

to a much darker pink than the supernatant. This effect was not observable for Pd-laden gels due to the dark black color of the Pd. The depletion of resorufin from the solution by the hydrogel discs was measured after 18 h and after 14 days, from which distribution coefficients (D_c) were calculated (**Figure 6**). For both hydrogel types, the dye concentration within the hydrogel was much higher than in the supernatant ($D_c \gg 1$), confirming the high affinity of the dye for the hydrogels as the driver for the dye reuptake. After 14 days, the D_c of pHEMA-co-AM was less than half that of pHEMA-GG (14.9 ± 0.9 versus 31.5 ± 1.2). This agrees with the higher final values for conversion and release of proresorufin for pHEMA-co-AM than for pHEMA-GG (Figure 4 versus Figure 3), and with the smaller ratio of sequestered dye released in the second 10-day period over the first 5-day period of leaching (Figure 5).

For pHEMA-GG, D_c increased with statistical significance from 18 h to 14 days, indicating equilibrium had not yet been reached after 18 h. In contrast, pHEMA-co-AM had reached equilibrium within 18 h; the D_c remained unchanged after 14 days. This confirms the faster diffusion of the dye through the pHEMA-co-AM copolymer compared with pHEMA-GG, which was also observed from the amounts of dye leached from discs exposed to proresorufin for the shortest duration of 0.5 h (Figure 5).

2.5. Catalysts Retain Activity over One Week with Daily Dosage

Next, the recyclability of the catalysts was investigated. Mimicking daily exposures after systemic administration of a prodrug, Pd-laden hydrogel discs were left in a prodye solution for 1 h, followed by 23 h in PBS between "dosages." This enabled investigation of the recyclability of the catalyst, but also if the sequestration of the dye by the hydrogels contributes to a more sustained release profile, whereby the hydrogel acts as a depot of converted product that would continue to release when prodrug is no longer offered in the bloodstream.

The release data from seven daily cycles (**Figure 7**) confirm that higher catalytic conversion and release were achieved when pHEMA-co-AM was used as the Pd carrier, compared with pHEMA-GG, for PdNC ($p < 10^{-8}$) as well as PdNS ($p = 0.0021$).
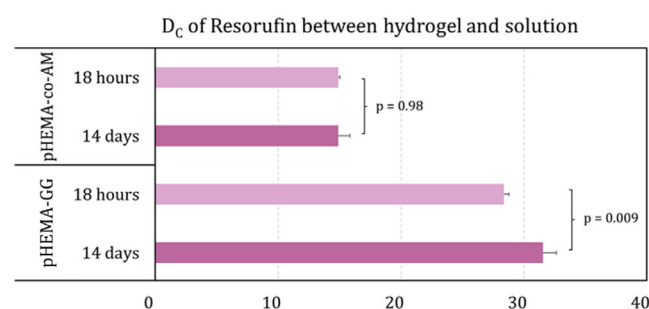
The higher activity of PdNS over PdNC is also confirmed for both pHEMA-GG ($p = 0.0002$) and pHEMA-co-AM ($p = 0.010$).

For all conditions, the activity decreased somewhat over the 7-day period. The decrease was more pronounced in pHEMA-GG than in pHEMA-co-AM, both in magnitude (1.63% versus 0.87% average loss per day) and in statistical significance (4 out of 5 pHEMA-GG samples showing a statistically significant downward trend in a Mann–Kendall test at $p < 0.05$, versus 2 out of 5 pHEMA-co-AM samples). The largest decrease is seen after the first day. In fact, when omitting the first day, there is no longer a statistically significant downward trend for the pHEMA-co-AM samples, and only for 1 out of 5 pHEMA-GG samples. With respect to recyclability, no trends can be discerned between the different nanoshapes.

The release over the 23 h periods in PBS in-between exposure to prodye was similar across all samples at $6.5 \pm 1.2\%$, with no differences between either polymer type or Pd nanoshape (confirmed by ANOVA). However, the release in the "off period" being independent of the catalytic activity meant that catalysts with lower activity during the 1 h periods showed more sustained release relative to those with higher activity. For example, for PdNC in pHEMA-GG, 33% of the total release was during the "off period," whereas for the other three groups this was 23–25%.
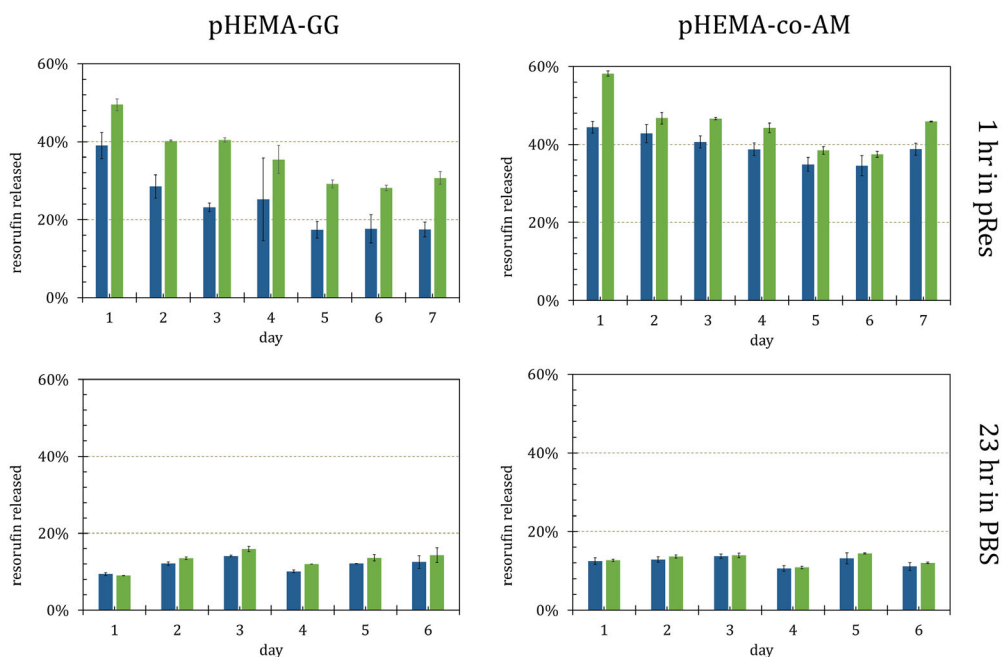
2.6. Nanosheets are Better Retained Inside Hydrogels than Nanocubes

Leaching of Pd from both pHEMA-GG and pHEMA-co-AM for both nanoshapes was measured indirectly, by assessing the catalytic activity of washings, that is, volumes of PBS in which the catalysts had been kept for set lengths of time. These washings were exposed to proresorufin under standard conditions, so the quantity of formed resorufin could be taken as a measure of amount of free Pd in each of the washings. A considerable loss of Pd was observed from both polymers functionalized with PdNC (**Figure 8**). For pHEMA-GG, the loss continued for up to 2 days, whereas loss from the copolymer diminished within the first hour. In contrast, loss of Pd was negligible from both polymers functionalized with PdNS.

3. Discussion

In this work, Pd nanocubes and nanosheets were formed in situ within poly(2-hydroxyethyl methacrylate) hydrogels of different hydrophilicities. The Pd nanocubes had a similar size and shape to those formed in solution, though the protocol was modified by omission of CTAB, the capping agent. This led to an improvement in catalytic activity, probably due to an improved reduction of Pd(II) into Pd(0) as inferred from the discs turning a deeper black. The Pd nanosheets prepared within the confined spaces inside the hydrogel networks were more irregularly shaped than those reported from solution preparations,[15,27–29] but still showed a 2D morphology, thus having a high specific surface area available for catalysis.

All heterogeneous catalysts were effective at catalyzing the bio-orthogonal uncaging of the model compound proresorufin into resorufin. Conversion and release were fast (apparent maxima were observed at 2 h) considering the mm-scale of the catalysts,

Figure 6. Concentration distribution ratios (D_C) of resorufin dye between hydrogel discs (1 mm) and PBS after 18 h (light pink) and 14 days (dark pink) showing higher affinity of dye for pHEMA-GG than for pHEMA-co-AM (monomer ratio 1:1.83). $N = 3$ discs × 3 fluorescence measurements = 9 measurements.

Figure 7. Catalyst recycling over 1 week with daily dosage. pHEMA-GG and pHEMA-co-AM (monomer ratio 1:1.83) discs with either PdNC (blue) or PdNS (green) were exposed to 49.5 μM proresorufin for 1 h per day, followed by 23 h leaching in PBS. Converted and released resorufin measured at the end of each 1 h period in the prodye solution (top row) showed higher activity for PdNS versus PdNC and for pHEMA-co-AM versus pHEMA-GG, with low loss of activity over time. Released resorufin measured after each 23 h period in PBS (bottom row) showed a similarly strong depot effect across polymer types and palladium nanoshapes. $N = 3$ or 2 discs $\times$ 3 fluorescence measurements $= 6$ or 9 measurements.
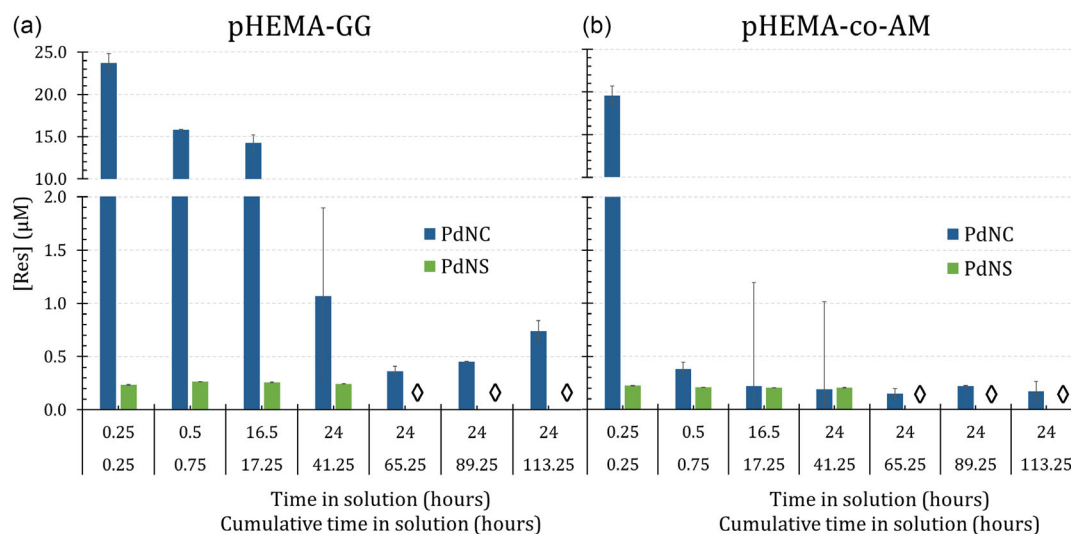
Figure 8. Concentration of resorufin converted from proresorufin by washings exposed to freshly prepared palladium-functionalized hydrogels. PdNS (green) washings showed minimal activity, while PdNC (blue) washings showed high initial activity, and slower decreases for a) pHEMA-GG than for b) pHEMA-co-AM (HEMA:AM = 1:1.83). Concentration of resorufin in solution (y-axis) is taken as proportional to the amount of palladium in solution after exposure to hydrogel discs for successive periods of time (x-axis). Diamond (◊) denotes PdNS-functionalized discs not assessed for these time-points. $N = 2$ discs $\times$ 2 washings $\times$ 3 fluorescence measurements $= 12$ measurements.

whereas most catalysts reported before were either micro- or nano-sized, that is, several orders of magnitude smaller.[10,13,14]

Between both nanoshapes, PdNS showed superior catalytic performance and better retainment within the hydrogels compared with PdNC. This is ascribed to the higher specific surface area of flat sheets compared with solid cubes. For example, the average PdNC of edge length 10.1 nm provides 612 nm² surface area at a volume of 1030 nm³, whereas the same volume of Pd in a nanosheet with a thickness of 0.3 nm (single atomic layer) would present an 11-fold higher surface area at 6,869 nm².

**ADVANCED
SCIENCE NEWS**

www.advancedsciencenews.com

**ADVANCED
NANOBIOMED
RESEARCH**
Open Access

www.advnanobiomedres.com

Between the polymers, the catalysts prepared within the pHEMA-co-AM copolymer showed faster diffusion, higher conversion, and release kinetics, as well as better recyclability than those prepared with pHEMA-GG. A significant difference between the polymers is hydrophilicity: pHEMA-GG is less hydrophilic (equilibrium swelling ratio of 2.00) than pHEMA-co-AM, which has a swelling ratio of 4.16 or 4.70 depending on the HEMA to acrylamide monomer ratio. The higher rates of conversion and release for the more hydrophilic polymer agree with earlier work on microbeads of different ratios of hydrophilic polyethylene glycol (PEG) to hydrophobic polystyrene (PS), where greater PEG/PS ratios yielded increased catalytic activity, as well as improved cell tolerance.[8] The data indicate that this is likely attributable to a difference in transport properties (diffusion rates and equilibrium partitioning constants) rather than a difference in the kinetics of catalysis at the surface of the Pd nanoshapes.

That same study observed that doxorubicin was sequestered from solution by the PEG/PS microbeads as it was produced by the Pd-catalyzed bioorthogonal uncaging of pro-doxorubicin. Attributed to the "lipophilic polystyrene core of the devices," this phenomenon was suggested to moderate interactions between the prodrug and embedded Pd nanoparticles and affect the product release.[8] This work investigated the phenomenon of this product sequestration in more detail, using hydrogels with different hydrophilicities and assessing release in the absence of prodye.

We found dye sequestration to be responsible for an apparently incomplete conversion in single kinetic experiments. This apparent decrease in conversion was exacerbated in thicker gels (higher volume ratio of polymer to supernatant) and in pHEMA-GG versus pHEMA-co-AM. Large amounts of dye were released from Pd-laden hydrogels after removal from the prodye solution, even after short incubation times with the prodye. Differences in release rates over subsequent periods revealed a higher affinity of the resorufin for pHEMA-GG than for pHEMA-co-AM, which was confirmed through uptake experiments of resorufin in Pd-free discs of both polymers. Resorufin is slightly lipophilic with an octanol/water partition coefficient of $10^{0.43} = 2.7$;[30] however, much higher affinities for the hydrogels were found in this study, with partition/concentration distribution coefficients of 14.9 for pHEMA-co-AM and 31.5 for pHEMA-GG. Dye uptake experiments further demonstrated that diffusion was faster in pHEMA-co-AM than in pHEMA-GG, which agreed with the faster conversion and release in the pHEMA-co-AM copolymer.

Our observations of product sequestration and delayed release suggest the potential of harnessing this behavior to control drug release. Exploiting such a "depot effect" could sustain the release of the active drug from the hydrogel within which it is converted, thereby extending the exposure of the tumor to the active chemotherapeutic between prodrug injections, thus enhancing its therapeutic potential. The application of such an implant would be two-fold: drug synthesis and subsequent sustained drug release. Through a cyclic experiment, where the catalysts were exposed to proresorufin for 1 h per day followed by a 23 h "off-period," we demonstrated the potential for this depot effect. Across all conditions, dye release in the off period was 23–33% of the total dye released. Although this is still far from proper sustained release

(as still 67–77% was released within only 1 h per day), it shows a potential that could be leveraged through the design of the heterogeneous catalyst. For example, one could envision a Pd-laden gel sandwiched between layers of Pd-free gel. This work demonstrates that at the hydrogel dimensions used (1 and 3 mm thickness), mass transport through the hydrogel is the rate-limiting factor, rather than the catalytic conversion by the Pd. The Pd-free layers would therefore act as a buffer, leading to a more sustained release profile. Although hydrogel-based sustained release drug delivery systems have been used and under development for years,[31] bioorthogonal chemistry could lead to a paradigm shift. It could enable the regular supply of new drug to the hydrogel depot in the form of an inert prodrug, as opposed to the current model where a finite amount of drug is present in the hydrogel depot and gets released over time. Combined with the already demonstrated advantages of improved bioavailability (including crossing the blood-brain barrier[4]) and reduced side effects, such control over dosage removes most of the current barriers to effective chemotherapy. Therefore, the further development of these catalysts holds promise to transform future cancer treatment. The stability and efficacy of Pd-doped hydrogels in biological systems should be evaluated over time to better understand their potential for clinical applications. Furthermore, the impact of the Pd-doped hydrogels on their resident biological systems needs to be further investigated, including potential toxicity of released Pd and the foreign body response which is likely to occur at the site of implantation.

4. Conclusion

In this work, we investigated the effect of Pd nanostructure shape and hydrogel hydrophilicity on the effectiveness of heterogeneous catalysts for bioorthogonal organometallic chemistry. Protocols for the synthesis of Pd nanocubes and Pd nanosheets were successfully adopted to form Pd nanoshapes in situ within hydrogels of different hydrophilicity. Using the fluorogenic model reaction of uncaging proparylated resorufin, Pd nanosheets showed superior catalytic activity over Pd nanocubes, as well as better retainment within the hydrogel with negligible leaching. Higher hydrophilicity of the polymer led to faster prodye conversion, higher release rates, and better recyclability. All polymers sequestered considerable amounts of converted product, which were subsequently released in the absence of proresorufin. This prodye uptake and release effect could be leveraged through catalyst design to apply to prodrug uptake and sustain the release of converted drugs to enhance the therapeutic effect of localized prodrug activation. It is anticipated that further development of these Pd-laden hydrogels will result in viable implants for bioorthogonal chemotherapy, promising to alleviate the side effects troubling current cancer treatment.

5. Experimental Section

Materials: 2-Hydroxyethyl methacrylate (HEMA), *N,N,N′,N′*-tetramethylethylenediamine (TEMED), palladium chloride (PdCl$_2$), potassium palladium(II) chloride (K$_2$PdCl$_4$), and cetyltrimethylammonium bromide (CTAB) were purchased from Sigma–Aldrich (Gillingham, UK). Ethylene glycol dimethacrylate (EGDMA), ammonium persulfate (APS), acrylamide

(AM), L-ascorbic acid (L-AA), and low acyl gellan gum were purchased from Alfa Aesar (Heysham, UK). Hydrochloric acid (HCl), potassium bromide (KBr), dimethylsulfoxide (DMSO), and phosphate-buffered saline (PBS) solution (10X) were purchased from Fisher Scientific (Loughborough, UK). Clear polyethylene terephthalate glycol (PETG) sheet (1 mm thick) was purchased from RS Components (UK). SuperGlue (Loctite, Henkel Corp., USA) was gifted by Tom Carvell (Heriot-Watt University). Resorufin (95% purity) was purchased from Fluorochem (UK), and propargylated-resorufin (proresorufin) was synthesized as previously described.[32] Resorufin and proresorufin stock solutions (5 mM in DMSO) were prepared by dissolution at 60 °C and stored at − 18 °C until required. All water used, denoted as dH$_2$O, was Ultrapure deionized water from Milli-Q tap. All chemicals were stored according to manufacturer guidelines. All chemicals were used as received, without any further purification.

Hydrogel Film Preparations: The methods below detail the preparation of prepolymerization mixture (7 g) to prepare two 1 mm films. When other amounts were required, all masses and volumes were scaled accordingly.

Hydrogel Film Preparations: Poly(2-Hydroxyethyl Methacrylate) (pHEMA-GG): pHEMA-GG was developed in a related study[33] where the granular gel facilitated the suspension of Pd-laden microbeads, and used here without said microbeads. Gellan gum granular gel (GG) was prepared as previously reported by shearing a 0.3 wt% gellan gum solution with an overhead stirrer as it cooled from 90 °C to room temperature and went through thermal gelation. APS (0.4564 g, 0.002 moles) was dissolved in GG (10 mL) by sonication to a final concentration of 0.2 M APS. Equal masses of HEMA and 0.2 M APS in GG were pipetted, followed by EGDMA, and mixed by gently inverting. The mixture was sonicated to remove bubbles. TEMED was added and the mixture was quickly mixed by inverting the vial several times initiating the polymerization, then transferred to film molds by pipette. Films were removed from the molds after 1 h and transferred to water or PBS, which was refreshed at 1 h intervals for 4–6 h, then daily for at least 5 days, to remove any molecules that may have washed out. The thickness of the films was measured using a thickness gauge, and the swollen films were cut into discs of 6 mm diameter using a biopsy punch. This material is referred to as **pHEMA-GG**.

Hydrogel Film Preparations: Poly(2-Hydroxyethyl Methacrylate-Co-Acrylamide) (pHEMA-co-AM): The protocol was loosely adapted from that reported in.[34] Where acrylamide (AM) was added as solution, it was prepared by dissolving solid AM monomer (10.78 g, 0.15 moles) in dH$_2$O (16.17 mL) yielding a final concentration of 40 wt% AM.

HEMA, AM, APS solution (in H$_2$O), and EGDMA were added to a vial, and gently inverted to mix before the addition of TEMED and transfer to 1 mm thick film molds by pipette, following the rest of the protocol as above, yielding hydrogel discs of **pHEMA-co-AM** (Table 1).

Preparation of Palladium Nanocubes: In solution: The protocol for batch synthesis of palladium nanocubes in solution was adapted from refs. [20,23]. Aqueous H$_2$PdCl$_4$ solution (0.5 mL, 10 mM) dissolved at 60 °C was added to CTAB solution (10 mL, 12.5 mM) and heated to 96 °C for 20 min. Freshly prepared L-AA solution (0.08 mL, 100 mM) was then quickly added under stirring and left undisturbed for 30 min. Cubic Pd nanoparticles were purified by two consecutive cycles of centrifugation (14 000 rpm, 20 min), cleaned with dH$_2$O between cycles, and redispersed in 10 mL of dH$_2$O.

In hydrogel discs: The above protocol was adapted for the synthesis of palladium nanocubes in situ in discs of pHEMA-GG and pHEMA-co-AM, with two approaches as described. Ten swollen hydrogel discs were submerged in H$_2$PdCl$_4$ (20 mL, 10 mM) at room temperature overnight, under gentle stirring. Then either:

The solution containing the discs was heated to 95 °C while stirred gently. After 60 min, the solution and discs were removed from the heat. Freshly prepared L-AA (0.16 mL per 2 mL H$_2$PdCl$_4$, 100 mM) was added.

The hydrogel discs were removed from H$_2$PdCl$_4$ solution, patted dry, and placed in a solution of CTAB (12.5 mM, 10.5 mL). This was heated to 95 °C under gentle stirring for 60 min. Once removed from heat, freshly prepared L-AA (0.56 mL, 100 mM) was quickly added.

After the addition of L-AA, the solutions were left undisturbed while cooling for 1 h, and then discs were recovered from solution, patted dry, and stored in PBS.

Preparation of Palladium Nanosheets: Swollen hydrogel discs of either pHEMA-GG or pHEMA-co-AM were left submerged in K$_2$PdCl$_4$ (7.5 mM)/KBr (0.15 M) solution overnight, at room temperature with gentle stirring. The discs were patted dry and kept separated inside a glass vial to enable mobility of the gas in and around the whole disc. The vial was placed inside the CO reactor at 6 bar CO for 40 min at 60 °C, adapted from previously published protocols.[12,25] Upon removal from the reactor, the Pd-discs were stored in PBS.

Imaging of Pd-Functionalized Hydrogel Samples: All image processing was done with ImageJ.

TEM and HAADF-STEM: Particle morphology and size distribution were determined using a T20-FEI Tecnai thermoionic Transmission Electron Microscope operated at 200 kV with a LaB6 electron source fitted with a "SuperTwin" objective lens allowing a point-to-point resolution of 2.4 Å. Hydrogel samples were prepared by fixing in epoxy to prepare a TEM grid by ultramicrotome (Leica EM UC7). Solution nanoparticles samples were prepared by dilution with Milli-Q water followed by 30 s sonication then casting of 5 µL on a holey carbon-supported TEM grid. Aberration-corrected scanning transmission electron microscopy (Cs-corrected STEM) images were acquired using a high-angle annular dark field detector in a FEI XFEG TITAN electron microscope operated at 300 kV equipped with a CETCOR Cs-probe corrector from CEOS Company allowing formation of an electron probe of 0.08 nm. Elemental analysis was carried out with an EDS (EDAX) detector which allows performing EDS experiments in the scanning mode. At least 200 particles were measured to evaluate the mean diameter of the particles and aspect ratio (length/width) distribution.

Prodye Conversion and Leaching Studies: All studies involving prodye conversion or leaching of dye or Pd were performed on swollen Pd-laden hydrogel discs placed individually in 1.5 mL microcentrifuge tubes. Proresorufin and resorufin were always used at a final concentration of 49.5 µM and samples containing it were kept in the dark to prevent photobleaching.

Prodye conversion and leaching: Discs in 1.00 mL PBS + 10 µL proresorufin stock were incubated in a Thriller thermoshaker (PEQLAB, Biotechnologie GMBH, Erlangen, Germany) at 1100 rpm shaking and 37 °C. Controls of resorufin (1.00 mL PBS + 10 µL resorufin stock) without disc were included. Discs were removed from the prodye solution at set times (0.5–18 h) and transferred to a 48-well plate in 1.00 mL PBS, kept

Table 1. Compositions of prepolymerization mixtures used for preparation of pHEMA-GG and pHEMA-co-AM hydrogels films using methods described above.

Material	HEMA monomer [wt%]	AM monomer [wt%]	diluent [wt%]	EGDMA crosslinker [wt%][a]	APS initiator [M]	TEMED co-initiator [M]
pHEMA-GG	50	–	50[b]	2	0.1	0.1
pHEMA-co-AM (1:1.83)	25	25[c]	50[d]	2	0.1[e]	0.1
pHEMA-co-AM (1:2.75)	20	30[f]	50[d]	2	0.14[g]	0.14

[a]wt% of total monomer mass; [b]0.3 wt% gellan gum granular gel; [c]Added as 40 wt% AM solution in H$_2$O; [d]PBS; [e]Added as 0.8M APS solution in H$_2$O; [f]Added as solid AM monomer; [g]Added as 0.2M APS solution in H$_2$O.

static for 5 days, and then transferred to a new well with 1.00 mL fresh PBS and kept static for another 10 days. The recyclability experiment was performed similarly, with each disc incubating in proresorufin on the thermoshaker for 1 h, followed by 23 h static leaching in a new tube with 1.00 mL PBS. This cycle was repeated seven times.

Pd leaching: As-prepared discs were kept in 1.00 mL PBS for a set time, before being transferred to the next vial with fresh PBS, and so on. Washings were diluted with 3.00 mL PBS, and 40 μL proresorufin stock was added. From this point onwards, the same procedure was followed as for the conversion studies, with 16 h incubation on the thermoshaker.

Detection: 3×100 μL per sample (tube or well) was pipetted into a black 96-well plate. A series of 7 concentrations from 0 to 49.5 μM resorufin were prepared by diluting the co-incubated resorufin control with PBS, in each individual 96-well plate for in situ calibration. Fluorescence intensities were measured on a POLARstar Omega plate-reader (BMG Labtech) at $\lambda_{ex} = 530$ nm and $\lambda_{em} = 590$ nm. A second-order polynomial calibration curve was fitted to the calibrated data points and used for converting fluorescent intensities of the samples into resorufin concentrations.

Determination of Resorufin Distribution Ratio between Hydrogel Discs and PBS: Swollen discs of pHEMA-GG and pHEMA-co-AM (monomer ratio 1:1.83) were placed individually in 1.5 mL microcentrifuge tubes in resorufin (1 mL, 101.2 μM) and incubated for 18 h on the thermoshaker-incubator as described above, followed by fluorescence intensity read-out as described above, including a 10-point calibration curve from 0 to 98 μM within the same plate prepared using a resorufin control incubated alongside the samples. In parallel, other samples were incubated at 37 °C without shaking for 14 days, followed by read-out in the same manner. The concentration distribution ratios (D_c) were calculated as $[Res]_{disc}/[Res]_{solution}$, accounting for the volumes of the discs and solutions.

Swelling of Hydrogel Discs: As-prepared discs were dried at 50–60 °C until mass was constant (m_{dry}) and left in PBS at room temperature until mass was constant (m_{sw}). Equilibrium swelling ratios were calculated as m_{sw}/m_{dry}.

Determination of Palladium Content: Discs were individually digested in 350 μL freshly prepared aqua regia (1:3 HNO_3:HCl) for 1 h at room temperature. The supernatant was filtered to remove any solid. Each sample was diluted 1:3 aqua regia:H_2O to a final volume of 1.4 mL. A 4100 microwave plasma atomic emission spectrometry (MP-AES) (Agilent Technologies, USA) was used to measure Pd content using commercial Pd sample as a standard.

Statistics: All values are reported as average ± standard deviation unless indicated otherwise. Reported p-values for head-to-head comparisons are obtained from two-tailed homoscedastic Student's T-test (MS Excel). Decreasing trends were tested for statistical significance using a Mann–Kendall test (XLSTAT).

Supporting Information

Supporting Information is available from the Wiley Online Library or from the author.

Acknowledgements

Conflict of Interest

The authors declare no conflict of interest.

Author Contributions

Data Availability Statement

The data that support the findings of this study are available from the corresponding author upon reasonable request.

Keywords

[1] H. C. Hang, C. Yu, D. L. Kato, C. Bertozzi, *Proc. Nat'l. Acad. Sci.* **2003**, *100*, 14846.

[2] B. Rubio-Ruiz, A. M. Pérez-López, L. Uson, M. Ortega-Liebana, T. Valero, M. Arruebo, J. Hueso, V. Sebastian, J. Santamaría, A. Unciti-Broceta, *Nano Lett.* **2023**, *23*, 804.

[3] J. T. Weiss, C. Fraser, B. Rubio-Ruiz, S. Myers, R. Crispin, J. Dawson, V. Brunton, E. Patton, N. Carragher, A. Unciti-Broceta, *Front. Chem.* **2014**, *2*, 56.

[4] C. Adam, T. L. Bray, A. M. Pérez-López, E. Tan, B. Rubio-Ruiz, D. Baillache, D. Houston, M. Salji, H. Leung, A. Unciti-Broceta, *J. Med. Chem.* **2022**, *65*, 552.

[5] J. T. Weiss, J. C. Dawson, C. Fraser, W. Rybski, C. Torres-Sanchéz, M. Bradley, E. Patton, N. Carragher, A. Unciti-Broceta, *J. Med. Chem.* **2014**, *57*, 5395.

[6] C. Adam, A. M. Pérez-López, L. Hamilton, B. Rubio-Ruiz, T. Bray, D. Sieger, P. Brennan, A. Unciti-Broceta *Chem. Eur. J.* **2018**, *24*, 16783.

[7] J. T. Weiss, N. O. Carragher, A. Unciti-Broceta, *Sci. Rep.* **2015**, *5*, 9329.

[8] T. L. Bray, M. Salji, A. Brombin, A. Pérez-López, B. Rubio-Ruiz, L. Galbraith, E. Patton, H. Leung, A. Unciti-Broceta, *Chem. Sci.* **2018**, *9*, 7354.

[9] G. M. Dal Forno, E. Latocheski, A. Beatriz Machado, J. Becher, L. Dunsmore, A. St. John, A. Oliveira, C. Navo, G. Jiménez-Osés, R. Fior, J. Domingos, G. Bernardes *J. Am. Chem. Soc.* **2023**, *145*, 10790.

[10] R. M. Yusop, A. Unciti-Broceta, E. M. V. Johansson, A. Unciti-Broceta, E. Johansson, R. Sánchez-Martín, M. Bradley, *Nat. Chem.* **2011**, *3*, 239.

[11] X. Zhang, R. F. Landis, P. Keshri, R. Cao-Milán, D. Luther, S. Gopalakrishnan, Y. Liu, R. Huang, G. Li, M. Malassiné, I. Uddin, B. Rondon, V. Rotello, *Adv. Healthc. Mater.* **2021**, *10*, 2001627.

[12] M. Sancho-Albero, B. Rubio-Ruiz, A. M. Pérez-López, V. Sebastián, P. Martín-Duque, M. Arruebo, J. Santamaría, A. Unciti-Broceta, *Nat. Catal.* **2019**, *2*, 864.

[13] J. T. Weiss, J. C. Dawson, K. G. Macleod, W. Rybski, C. Fraser, C. Torres-Sánchez, E. Patton, M. Bradley, N. Carragher, A. Unciti-Broceta, *Nat. Commun.* **2014**, *5*, 3277.

[14] A. Unciti-Broceta, E. M. V. Johansson, R. M. Yusop, R.Sánchez-Martín, M. Bradley, *Nat. Protoc.* **2012**, *7*, 1207.

[15] A. M. Pérez-López, B. Rubio-Ruiz, T. Valero, R. Contreras-Montoya, L. Álvarez de Cienfuegos, V. Sebastián, J. Santamaría, A. Unciti-Broceta, *J. Med. Chem.* **2020**, *63*, 9650.

[16] M. C. Ortega-Liebana, N. J. Porter, C. Adam, T. Valero, L. Hamilton, D. Sieger, C. Becker, A. Unciti-Broceta, *Angew. Chem. Int. Ed.* **2022**, *61*, e202111461.

[17] Q. Zhang, F. Li, L. Lin, J. Peng, W. Zhang, W. Chen, Q. Xiang, F. Shi, W.Shang, P. Tao, C. Song, R. Huang, H. Zhu, T. Deng, J. Wu, *ChemElectroChem* **2020**, *7*, 2614.

[18] E. Dahal, J. Curtiss, D. Subedi, G. Chen, J. Houston, S. Smirnov, *ACS Appl. Mater. Interfaces* **2015**, *7*, 9364.

[19] R. Long, K. Mao, X. Ye, W. Yan, Y. Huang, J. Wang, Y. Fu, X. Wang, X. Wu, Y. Xie, Y. Xiong, *J. Am. Chem. Soc.* **2013**, *135*, 3200.

[20] W. Niu, Z.-Y. Li, S. Shi, X. Liu, H. Li, S. Han, J. Chen, G. Xu, *Cryst. Growth Des.* **2008**, *8*, 4440.

[21] J.-S. Ye, C.-W. Chen, C.-L. Lee, *Sens. Actuators, B* **2015**, *208*, 569.

[22] S. Swain, M. B. Bhavya, V. Kandathil, B. Phol, A. Samal, S. Patil, *Langmuir* **2020**, *36*, 5208.

[23] A. Pekkari, Z. Say, A. Susarrey-Arce, C. Langhammer, H. Härelind, V. Sebastián, K. Moth-Poulsen, *ACS Appl. Mater. Interfaces.* **2019**, *11*, 36196.

[24] L. Uson, C. Yus, G. Mendoza, E. Leroy, S. Irusta, T. Alejo, D. García-Domingo, A. Larrea, M. Arruebo, R. Arenal, V. Sebastián, *Adv. Funct. Mater.* **2022**, *32*, 2106932.

[25] V. Sebastian, M. Sancho-Albero, M. Arruebo, A. Pérez-López, B. Rubio-Ruiz, P. Martin-Duque, A. Unciti-Broceta, J. Santamaría, *Nat. Protoc.* **2021**, *16*, 131.

[26] V. Sebastián, K. F. Jensen, *Nanoscale* **2016**, *8*, 15288.

[27] X. Huang, S. Tang, X. Mu, Y. Dai, G. Chen, Z. Zhou, F. Ruan, Z. Yang, N. Zheng, *Nat. Nanotechnol.* **2011**, *6*, 28.

[28] V. Sebastian, C. D. Smith, K. F. Jensen, *Nanoscale* **2016**, *8*, 7534.

[29] L. Herrer, V. Sebastian, S. Martín, A. González-Orive, F. Pérez-Murano, P. Low, J. Serrano, J. Santamaría, P. Cea, *Nanoscale* **2017**, *9*, 13281.

[30] B. Hee Han, M. Zhou, A. K. Vellimana, E. Milner, D. Kim, J. Greenberg, W. Chu, R. Mach, G. Zipfel, *Mol. Neurodegener.* **2011**, *6*, 86.

[31] J. C. Quarterman, S. M. Geary, A. K. Salem, *Eur. J. Pharm. Biopharm.* **2021**, *159*, 21.

[32] B. Rubio-Ruiz, A. M. Pérez-López, T. L. Bray, M. Lee, A. Serrels, M. Prieto, M. Arruebo, N. Carragher, V. Sebastián, A.Unciti-Broceta, *ACS Appl. Mater Interfaces.* **2018**, *10*, 3341.

[33] A. McGuigan, F. Melchels, Palladium Nanoparticles in Hydrogels for Catalytic Prodrug Activation and Controlled Drug Release. Tissue Engineering and Regenerative Medicine Inter. Society (TERMIS) European Chapter Conf. Krakow, Poland **2022**.

[34] S. Kim, B. Shin, C. Yang, S. Jeong, J. Shim, M. Park, Y. Choy, C. Heo, K.Lee, *Polymers* **2018**, *10*, 772.